Accepted Manuscript

Electrochemical biosensing of influenza A subtype genome based on meso/ macroporous cobalt (II) oxide nanoflakes-applied to human samples

J. Mohammadi, A. Moattari, N. Sattarahmady, N. Pirbonyeh, H. Yadegari, H. Heli

PII: S0003-2670(17)30602-5

DOI: 10.1016/j.aca.2017.05.010

Reference: ACA 235220

To appear in: *Analytica Chimica Acta*

Received Date: 5 March 2017

Revised Date: 5 May 2017

Accepted Date: 12 May 2017

Please cite this article as: J. Mohammadi, A. Moattari, N. Sattarahmady, N. Pirbonyeh, H. Yadegari, H. Heli, Electrochemical biosensing of influenza A subtype genome based on meso/macroporous cobalt (II) oxide nanoflakes-applied to human samples, *Analytica Chimica Acta* (2017), doi: 10.1016/ j.aca.2017.05.010.

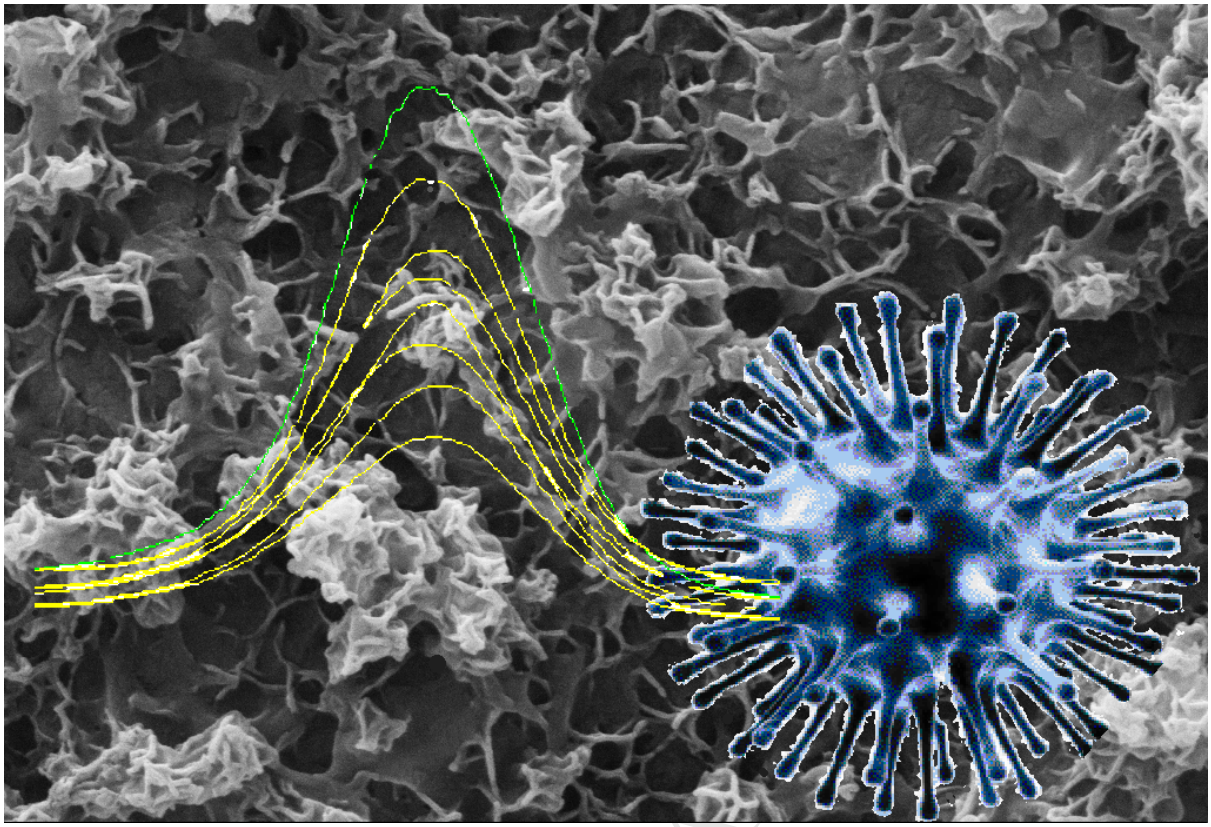

Electrochemical biosensing of influenza A subtype genome based on meso/macroporous cobalt (II) oxide nanoflakes-applied to human samples

J. Mohammadi [a,b], A. Moattari [a], N. Sattarahmady [b,c], N. Pirbonyeh [a], H. Yadegari [d], H. Heli [b]*

[a] Microbiology, Bacteriology and Virology Department, School of Medicine, Shiraz University of Medical Sciences, Shiraz, Iran
[b] Nanomedicine and Nanobiology Research Center, Shiraz University of Medical Sciences, Shiraz, Iran
[c] Department of Medical Physics, School of Medicine, Shiraz University of Medical Sciences, Shiraz, Iran
[d] Department of Mechanical and Materials Engineering, University of Western Ontario, London, Ontario N6A 5B9, Canada

*Corresponding author. E-mail: hheli7@yahoo.com, heli@sums.ac.ir (H. Heli), Tel: +98 71 36 12 22 25,6; Fax: +98 71 36 28 15 06.

Abstract

Meso/macroporous cobalt (II) oxide nanoflakes were electrodeposited in a one-step process in the presence of N-methylpyrrolidone. On the surface of nanoflakes, a specific single stranded DNA sequence from the genome of influenza A subtype was then immobilized to fabricate an electrochemical biosensor. Hybridization of the biosensor with complementary, non-complementary and base-mismatch sequences was electrochemically detected. The biosensor was also employed to detect complementary DNA of viral RNA in culture and human samples. The biosensor could detect the complementary sequence with a detection limit of 86.4 amol L^{-1} and a linear concentration range of 1.0 fmol L^{-1} to 1.0 nmol L^{-1}. It also detected a complementary DNA sequence converted from viral RNA with a detection limit of 0.28 ng μL^{-1} in a linear concentration range of 0.5 to 10 ng μL^{-1}. Low detection limit, simple method of preparation of the transducer and no needing any DNA strand modification and tag are the principal advantages of the biosensor.

Keywords: Influenza; Genosensor; DNA biosensor; CoO; Nanoflake; Cobaltous oxide

1. Introduction

Detection of DNA hybridization is important in various areas such as disease diagnosis, gene therapy, pathogens detection, and biological and medical studies [1-4]. Using a unique DNA sequence, we can design high sensitive and selective biosensors for the detection of different infectious microorganism including bacteria, viruses and parasites based on DNA hybridization [3-7] and detection of proteins, small molecules and metal ions [8, 9]. For the DNA hybridization biosensing, different detection systems of surface plasmon resonance, quartz crystal microbalance, immunoassays, UV-vis spectroscopy [3] and electrochemical methods [4, 5] have been employed. Signal transduction in DNA hybridization biosensors working electrochemically contains

different strategies of redox behavior of the nucleic acid [10], DNA intercalators and groove binders [5, 8], enzyme labels [11], and metal nanostructure tags [12]. Electrochemical biosensors with the advantages of high sensitivity and low detection limit, high accuracy, inexpensive and small dimensions have applications in a variety of areas [2, 4-8].

For the fabrication of DNA biosensors, the key step is the immobilization of a specific single stranded DNA (ssDNA) sequence on the transducer surface. For the transducers, nanomaterials are the recent choice due to the high surface area to volume ratio, and providing a high surface concentration of the immobilized ssDNA. This later effect leads to high-sensitive DNA biosensors. Additionally, nanostructured materials affect the hybridization medium causing increment in the selectivity and further signal amplification [4, 5, 7, 8, 13]. In this regard, various nanomaterials of magnetic [4], carbon [14], metals and semiconductors [3, 15], conducting polymers [16] and metal oxides [4, 17-20] have been utilized to fabricate DNA biosensors.

Influenza is an acute respiratory disease caused by influenza virus ranging from common cold to severe pneumonia. History of the flu virus goes back to the time of Hippocrates, and up to now, it has had a significant impact on human health. High mortality of the disease and high genetic variation of the virus have made it a unique one in viral infections. Annually, >250,000 deaths occur due to influenza, and rapid and sensitive detection of the diseases is critical.

There are methods of influenza virus detection including virus isolation in cell cultures (as a gold standard method) [21], immuno- (e.g. immuno-fluorescence) assays, compliment fixation, hemagglutination-inhibition assay, PCR and biosensors [22-27]. Cell culture has the limitations of long duration, restrictions in virus replication and need to experienced personnel, compliment fixation with low specificity, and need for much time and experienced personnel. Also, hemagglutination inhibition assay needs to remove non-specific inhibitors, and PCR requires enough time, experienced personnel and considerable cost and produces false positive tests. For biosensing influenza virus, different methods are used to detect DNA sequences that include radiochemical, enzymatic, fluorescent, electrochemical, optical, and acoustic wave. Among them, DNA detection by electrochemical methods is more attended.

In the present study, a simple, low-cost and sensitive electrochemical biosensor was designed for the detection of influenza A subtype in clinical samples using meso/macroporous cobaltous oxide nanoflakes without using any DNA probe modification, label, or tag.

2. Materials and methods

2.1. Materials

All chemicals were of analytical grade from Merck (Germany) or Sigma (USA) and were used without further purification. All solutions were prepared with redistilled water. A 21-mer synthetic oligonucleotide probe (pDNA) was designed based on the genomic sequence in influenza A subtype virus using Primer 3 and Primer Blast softwares. pDNA was selected from M gene of A/California/01/2009 (H1N1) (GenBank accession no. GQ475895.1). The sequence of pDNA was evaluated for any possible homology and share sequences with other subtypes of influenza virus using the BLAST software. The melting temperature of pDNA was also placed within a narrow range using the Oligo

software. The pDNA sequence was evaluated for potential self-dimmer and formation of secondary structures using mfold software, too. A complementary-sequence oligonucleotide (target oligonucleotide, a 21-base fragment of influenza virus gene sequence, tDNA) and a non-complementary sequence oligonucleotide (ncDNA) and base mismatched sequences were also designed. All the oligonucleotide sequences were purchased from Metabion Co. (Germany). The oligonucleotide sequences are as follows:

pDNA sequence: 5'GGT TTT GGC CAG CAC TAC AGC3'
tDNA sequence: 5'CCA AAA CCG GTC GTG ATG TCG3'
one-base mismatch sequence (1miss): 5'CTA AAA CCG GTC GTG ATG TCG3'
two-base mismatch sequence (2miss): 5'CCA AAA CAA GTC GTG ATG TCG3'
three-base mismatch sequence (3miss): 5'CCA AAA TCG ATC ATG ATG TCG3'
ncDNA sequence: 5'TAT GGA GAG TTT GAT CCT CGC TC3'

The oligonucleotide stock solutions were prepared with deionized water and kept at 4 °C.

2.2. Apparatus

Electrochemical tests were done in a three-electrode cell connected to a μ-Autolab potentiostat/galvanostat (the Netherlands). An Ag/AgCl, 3 mol L^{-1} KCl, a platinum rod, and a meso/macroporous cobaltous oxide nanoflakes-modified platinum disk (CoO/Pt) electrode (2 mm of diameter) were used as the reference, counter and working electrodes, respectively. GPES 4.9 software was run the system.

Field emission scanning electron microscopy (FESEM) was carried out by a Zeiss, Sigma-IGMA/VP (Germany) with the capability of energy-dispersive X-ray spectroscopy (EDS). For the sample preparation, a 2-5 nm thin film of gold was sputtered.

2.3. Preparation of the CoO/Pt electrode

CoO/Pt electrode was prepared similar to that reported elsewhere [28] with a modification of N-methylpyrrolidone employment as an additive. Before electrodeposition of meso/macroporous cobaltous oxide nanoflakes, the platinum disk electrode was cleaned by a sand paper and a polishing pad of 0.05 μm-alumina powder lubricated by water until a mirror-like gold surface was attained. Then, the electrode was immersed in a 1:3 water/ethanol mixture and ultrasonicated for 8 min in an ultrasound bath. The platinum disk electrode was then immersed in the synthesis solutions comprising 7.0 mL 0.1 mol L^{-1} $Co(NO_3)_3$ in water + 3 mL N-methylpyrrolidone. Electrodeposition of meso/macroporous cobaltous oxide nanoflakes was performed at -1000 mV for 60s without stirring the solution. The CoO/Pt electrode was then rinsed thoroughly with distilled water.

2.4. Immobilization of pDNA on the CoO/Pt electrode surface

Immobilization of pDNA was performed by dropping 10.0 μL of 10.0 μmol L^{-1} pDNA solution on the CoO/Pt electrode surface and kept at room temperature to dry [4]. Then, the electrode was rinsed with 20 mmol L^{-1} Tris-HCl buffer, pH 7.4 solution (Tris) to remove unspecific adsorbed pDNA. The obtained electrode was denoted as the biosensor.

2.6. Hybridization

The hybridization process was performed by immersing the biosensor into Tris containing various concentrations of tDNA. The time and temperature of the hybridization process were 40 min and 37 °C, respectively [4]. Then, the electrode was rinsed with Tris to remove the un-hybridized tDNA, and then it was incubated in a solution containing Tris + NaCl (20 mmol L^{-1}) + methylene blue (MB, 20 mmol L^{-1}). Time and temperature of incubation were 5 min and room temperature, respectively. The electrode was then rinsed with Tris to eliminate the physically adsorbed MB.

2.7. Electrochemical measurements

Electrochemical hybridization detection was carried out in 10 mL Tris, and differential pulse voltammograms (DPVs) were recorded for the MB reduction reaction. The instrumental parameters were pulse width of 25 mV, a pulse time of 50 ms, and a scan rate of 10 mV s^{-1}. The concentration of tDNA was quantified as the MB reduction peak currents in DPVs.

2.8. Cell culture, viral RNA extraction, and human samples

Madin-Darby canine kidney (MDCK) cells were purchased from Pasteur Institute (Iran). The cells were culture in Dulbecco's Modified Eagle's medium (DMEM) received from Sigma (USA) containing 10% fetal bovine serum received from Gibco (USA) and 100 units mL^{-1} penicillin and 100 μg mL^{-1} streptomycin received from Sigma (USA) at 37 °C in a humidified 5% CO_2 atmosphere. MDCK cells and 2 μg mL^{-1} TPCK was used for viral replication of influenza virus A/California/01/2009(H1N1).

Viral genomic RNA was extracted from the cultured cells by a High Pure Viral RNA Kit from Roche Co. (Germany). Viral RNA was then converted to the complementary DNA (cDNA) using a 2-step reverse transcription PCR Kit from Vivantis Co. (Malaysia). This kit was specially designed to provide reliable synthesis of full-length cDNA and convenient application of cDNA in PCR. M-MuLV, RNase H- synthesizes cDNA strand, initiating from a specific primer and random hexamer. Matrix gene was then amplified by PCR using the following primers:

Forward primer: 5'GAC GAA CGG AAT TTT TCC AAT CCC3'

Reverse primer: 5'TGC CGA TCA CTT AAG GGC CTT CAT3'

Matrix gene of influenza A was amplified by PCR. The reaction mixture was made up to final volume of 50 μL containing 1×PCR buffer purchased from Cinnagen (Iran), 0.2 μM dNTP, 1 μL of 10 pmol μL^{-1} primers, 1.5 Units of Taq polymerase, 1.5 μM of $MgCl_2$, and 5 μL of cDNA. The reaction mixtures were amplified in a thermal cycler from Eppendorf Inc (USA) at 95 °C for 5 min; this was followed by 35 cycles at 95 °C for 45 s, 55 °C for 40 s, 72 °C for 45 s, and one final extension at 72 °C for 3 min. 8 μL of the amplified reaction mixture was taken and fractionated in a 2% agarose gel containing TAE buffer 1× (100 mmol L^{-1} Tris-HCl pH 8.0, 90 mmol L^{-1} Acetic acid, 1 mmol L^{-1} Na-EDTA), stained with a safe stain from YTA Co. (IRAN), and visualized under UV light. To measure the concentration of the cDNA samples, Thermo Scientific NanoDrop 2000c (USA) was employed.

Negative control (non-template control) was included in each run and results were assumed valid only if all negative controls showed no band in electrophoresis step. PCR results were accepted as positive when a clear band was detected at the expected sizes. PCR produces 204 base pairs for matrix gene of influenza A.

Human swab samples were received from Emam Reza Hospital (Iran). The samples were transfered on ice to the lab, and RNA was extracted from the samples by a High Pure Viral RNA Kit from Roche Co. (Germany). Each sample of RNA was tested by separate primer/probe sets for the detection and copy number determination of influenza A by real-time PCR (RT-PCR). According to the CDC real-time PCR protocol (2009), the cycling conditions included a 30 min real-time step at 50 °C, followed by enzyme inactivation at 95 °C for 2 min. The PCR step comprised 45 cycles at 95 °C for 15 s, 55 °C for 30 s, and 72 °C for 30 s. Data acquisition and analysis of the RT-PCR assay were accomplished using the Rotor-Gene data analysis Software 6.0A. RT-PCR was carried out using SuperScript III Platinum one-step quantitative RT-PCR kit received from Invitrogen (USA). Real-time runs were performed on the Corbett 6000 Rotor-Gene system. The reaction comprised 4 μL of the extracted RNA combined with 16 μL of the master mix, including 2× reaction mix; SuperScript III RT/Platinum Taq Mix; 5.4 μL RNase/DNase-Free water; and 0.4 μL of each primer and probe with 40 μL and 10 μL, respectively. cDNA samples were heated at 90 °C for 5 min to unzip to ssDNA. Ethical Committee license number was 94-7563.

3. Results and discussion

FESEM images of different magnifications and an EDS spectrum from the CoO/Pt electrode surface are presented in Fig. 1 and supplementary material S1. Nanoflakes with high meso/macroporousities covered the entire surface with a mean size of 15±5 nm (n=150). The purity and the stoichiometry of the nanoflakes to be high purity cobaltous oxide were approved by EDS. When a highly negative potential of -1000 mV is applied to the working electrode, local medium near the electrode surface becomes alkaline due to water reduction reaction, and cobalt ions precipitate on the electrode surface. Compared to the cobaltous oxide nanoflakes synthesized in the absence of N-methylpyrrolidone [28], it seems that this additive induced softer layers with smaller thickness and interlayer distance.

As a transducer, the meso/macroporous structure of the nanoflakes provides a high specific surface area, and therefore, it can provide a high surface concentration of the immobilized pDNA and a shorter length of diffusion. This structure can also alter the immobilized pDNA configuration to a more suitable state for hybridization with tDNA. An enhancement in the hybridization process to form the double stranded DNA (dsDNA) will be the result [5, 29]. As for the immobilization capability of cobaltous oxide, it should be noted that the hydrated form of this oxide ($Co(OH)_2$) has an isoelectric point of 11±0.2 [30]. Therefore, after immersion of the nanoflakes into Tris, they adsorb pDNA through electrostatic attractions between positive surface charge of the CoO/Pt electrode and negative phosphate group at the 5’ end of pDNA. Although this route of immobilization may be altered by ionic strength of the medium, the very simple method of deposition, no need to functionalizing pDNA, and no need to any tag or marker are the advantaes of this immobilization route.

Fig. 2 shows DPVs for MB recorded using the biosensor, and after hybridization with tDNA of different concentrations. MB can bind to either ssDNA or dsDNA by electrostatic attractions and/or intercalation [31]. It depends on the ionic strength of the surrounding medium. The ionic strength of Tris makes favorable MB binding to the

guanine bases of pDNA [32] by stacking (hydrophobic interaction) of aromatic structures of MB and guanine. In DPVs presented in Fig. 2, the peak current was continuously decreased upon further hybridization and linearly depended on the tDNA concentration with a calibration plot presented in Fig. 2, inset. Based on the calibration plot, a regression equation of $y = -(0.2032\pm0.0048)x - (0.6572\pm0.0588)$ with a linear range of 1.0 fmol L^{-1} to 1.0 nmol L^{-1} for tDNA concentration was obtained. The limit of detection (LOD) of the biosensor was acquired based on the 3σ criterion, where σ is the standard deviation of the blank signal (n=5) as 86.4 amol L^{-1} of tDNA. A comparison between different electrochemical biosensors for influenza virus is performed in Table 1. Based on the information presented in this Table, the fabrication of the present biosensor was very simple, was applied to the analysis of human samples, and had the lowest detection limit.

In order to detect cDNA of influenza genome, viral RNA was extracted from the culture medium, converted to cDNA, and the cDNA concentrations in the samples were obtained. Solutions of cDNA of different concentrations were then prepared and placed at 90 °C for 5 min to unzip. Subsequently, DPVs were recorded for these solutions and they are depicted in Fig. 3. A calibration plot for the dependency of the peak currents on the cDNA concentration is shown in Fig. 3, inset. The regression equation of the calibration plot is $y = -(1.4372\pm0.0127)x + (2.3205\pm0.0079)$ and a LOD value of 0.28 ng μL^{-1} was achieved.

As for check the selectivity of the biosensor, 1miss, 2miss, 3miss and ncDNA sequences of 1.0×10^{-12} mol L^{-1} as negative controls were hybridized. DPVs recorded for these sequences are displayed in Fig. 4. In these DPVs, the peak current for ncDNA sequence is almost the same as pDNA, and the current was decreased upon increment in the similarity of these sequences to tDNA, i.e. $I_{p,pDNA}\approx I_{p,ncDNA}>I_{p,3miss}>I_{p,2miss}>I_{p,1miss}>I_{p,tDNA}$ (where I_p is the DPV peak current). Therefore, the biosensor could discriminate just one base mismatch in the hybridization sequence, and it can be considered as selective.

The biosensor regeneration was estimated by a five cycles of hybridization/dehybridization of tDNA of 1.0×10^{-12} mol L^{-1}, while between each cycle the biosensor was placed at 90 °C for 5 min to dehybridize. Fig. 5 exhibits DPVs for these cycles, and based on the results, the peak current measured for the biosensor after hybridization cycles had a slight change with a relative standard deviation (RSD) of 4.3%. The biosensor was stored in Tris when not in use and its activity was retained at least for 3 weeks.

In order to apply the biosensor for the detection of influenza virus in human samples, the corresponding cDNA samples from 7 patients and 4 healthy persons were analyzed. Qualitatively, the decrements in the peak currents after hybridization of the biosensor with cDNA from healthy persons were the same as that for pDNA, or smaller than $10\times\sigma$; that is, the differences between the values of the peak current were not significant. By contrast, the decrements in the peak currents after hybridization of the biosensor with cDNA from patients were higher than $10\times\sigma$, confirming the presence of viral RNA in the patient samples. Quantitatively, the concentrations of cDNA in the patient samples were measured using the previously plotted calibration curve, reported in Table 2, and compared to the values obtained from optical density measurements. The obtained results indicated that this simple, low-cost and sensitive electrochemical biosensor is able to detect influenza virus type A in samples from patients.

4. Conclusion

A simple electrodeposition route was developed to produce cobaltous oxide nanoflakes with a meso/macroporous structure in one step. The nanoflakes have a net positive surface charge and can adsorb a specific (negatively charged) ssDNA probe to fabricate a very simple electrochemical influenza A DNA biosensor. The biosensor is simply fabricated, label-free and low-cost. Other additives can alter the structure of cobaltous oxide, and using another specific DNA probes, we can develop this biosensor to another subtype and/or serotype of influenza.

Acknowledgments

The paper has been extracted from the J. Mohammadi M. Sc. thesis supported by the Research Council of Shiraz University of Medical Sciences (94-7563).

References

[1] A. Zinchenko, DNA conformational behavior and compaction in biomimetic systems: Toward better understanding of DNA packaging in cell, Advances in Colloid and Interface Science, Volume 232, June 2016, Pages 70-79.

[2] H. Heli, A.A. Moosavi-Movahedi, A. Jabbari, F. Ahmad, An electrochemical study of safranin O binding to DNA at the surface, J. Solid State Electrochem. 11 (2007) 593-599.

[3] N. Sattarahmady, G.H. Tondro, M. Gholchin, H. Heli, Gold nanoparticles biosensor of Brucella spp. genomic DNA: Visual and spectrophotometric detections, Biochem. Engin. J. 97 (2015) 1-7.

[4] H. Heli, N. Sattarahmady, G.R. Hatam, F. Reisi, R. Dehdari Vais, An electrochemical genosensor for Leishmania major detection based on dual effect of immobilization and electrocatalysis of cobalt-zinc ferrite quantum dots, Talanta 156-157 (2016) 172-179.

[5] A. Rahi, N. Sattarahmady, H. Heli, Zepto-molar electrochemical detection of Brucella genome based on gold nanoribbons covered by gold nanoblooms, Sci. Rep. 5 (2015) 18060.

[6] D.J. Chung, K.C. Kim, S.H. Choi, Electrochemical DNA biosensor based on avidin-biotin conjugation for influenza virus (type A) detection, Applied Surface Science 257 (2011) 9390-9396.

[7] A. Rahi, N. Sattarahmady, H. Heli, An ultrasensitive electrochemical genosensor for Brucella based on palladium nanoparticles, Anal. Biochem. 510 (2016) 11-17.

[8] A. Rahi, N. Sattarahmady, H. Heli, Label-free electrochemical aptasensing of the human prostate-specific antigen using gold nanospears, Talanta 156-157 (2016) 218-224.

[9] A. Bala, L. Gorski, Application of nucleic acid analogues as receptor layers for biosensors, Anal. Methods 8 (2016) 236-244.

[10] K. Kerman, Y. Morita, Y. Takamura, E. Tamiya, Escherichia coli single-strand binding protein-DNA interactions on carbon nanotube-modified electrodes from a label-free electrochemical hybridization sensor, Anal. Bioanal. Chem. 381 (2005) 1114-1121.

[11] D. Hernandez-Santos, M. Diaz-Gonzalez, M.B. Gonzalez-Garcia, A. Costa-Garcia, Enzymatic genosensor on streptavidin-modified screen-printed carbon electrodes, Anal. Chem. 76 (2004) 6887-6893.
[12] R. Bakalova, Z. Zhelev, H. Ohba, Y. Baba, Quantum dot-conjugated hybridization probes for preliminary screening of siRNA sequences, J. Am. Chem. Soc. 127 (2005) 11328-11335.
[13] J.H. Liu, J.Y. Liu, L.B. Yang, X. Chen, M.Y. Zhang, F.L. Meng, T. Luo, M.Q. Li, Nanomaterial-assisted signal enhancement of hybridization for DNA biosensors: a review, Sensors 9 (2009) 7343-7346.
[14] A. Erdem, Nanomaterial-based electrochemical DNA sensing strategies, Talanta 74 (2007) 318-325.
[15] F. Wang, S. Hu, Electrochemical sensors based on metal and semiconductor nanoparticles, Microchim. Acta 165 (2009) 1-22.
[16] H. Peng, L. Zhang, C. Soeller, J. Travas-Sejdic, Conducting polymers for electrochemical DNA sensing, Biomater. 30 (2009) 2132-2148.
[17] M. Chen, C. Hou, D. Hou, M. Yang, H. Fa, An ultrasensitive electrochemical DNA biosensor based on a copper oxide nanowires/single-walled carbon nanotubes nanocomposite, Appl. Surf. Sci. 364 (2016) 703-709.
[18] H. Zhu, J. Wang, G. Xu, Fast synthesis of Cu2O hollow microspheres and their application in dna biosensor of hepatitis B virus, Crystal Growth Design 9 (2009) 633-638.
[19] S.C. Sultan, P. Kara, U. Anik, M. Ozsoz, Label and indicator free electrochemical nanobiosensing of DNA hybridization based on MnO2 nanomaterial modified GCPE, RSC Adv. 4 (2014) 39691-39696.
[20] S. Mohan, P. Srivastava, S.N. Maheshwari, S. Sundar, R. Prakash, Nano-structured nickel oxide based DNA biosensor for detection of visceral leishmaniasis (Kala-azar), Analyst 136 (2011) 2845-2851.
[21] G.D. Hsiung, Diagnostic virology: from animals to automation, Yale J. Biol. Med. 57 (1984) 727-733.
[22] Y. Fu, Z. Callaway, J. Lum, R. Wang, J. Lin, Y. Li, Exploiting enzyme catalysis in ultra-low ion strength media for impedance biosensing of avian influenza virus using a bare interdigitated electrode, Anal. Chem. 86 (2014) 1965-1971.
[23] S. Aydinlik, D. Ozkan-Ariksoysal, P. Kara, A.A. Sayiner, M. Ozsoz, A nucleic acid-based electrochemical biosensor for the detection of influenza B virus from PCR samples using gold nanoparticle-adsorbed disposable graphite electrode and Meldola's blue as an intercalator, Anal. Methods 3 (2011) 1607-1614.
[24] A. Bonanni, M.I. Pividori, M. del Valle, Impedimetric detection of influenza A (H1N1) DNA sequence using carbon nanotubes platform and gold nanoparticles amplification, Analyst 135 (2010) 1765-1772.
[25] P.D. Tam, N.V. Hieu, N.D. Chien, A.T. Le, M.A. Tuan, DNA sensor development based on multi-wall carbon nanotubes for label-free influenza virus (type A) detection, J. Immun. Methods 350 (2009) 118-124.
[26] K. Malecka, A. Stachyra, A. Gora-Sochacka, A. Sirko, W. Zagorski-Ostoja, H. Radecka, J. Radecki, Electrochemical genosensor based on disc and screen printed goldelectrodes for detection of specific DNA and RNA sequences derivedfrom Avian Influenza Virus H5N1, Sens. Actuat. B 224 (2016) 290-297.

[27] Y. Amano, Q. Cheng, Detection of influenza virus: traditional approaches and development of biosensors, Anal. Bioanal. Chem. 381 (2005) 156-164.
[28] H. Heli, H. Yadegari, Nanoflakes of the cobaltous oxide, CoO: Synthesis and characterization, Electrochim. Acta 55 (2010) 2139-2148.
[29] L. Soleymani, Z. Fang, E.H. Sargent, S.O. Kelley, Programming the detection limits of biosensors through controlled nanostructurin, Nature Nanotechnol 4 (2009) 844-848.
[30] H. H. Kung, Transition Metal Oxides, Vol. 45: Surface Chemistry and Catalysis Elsevier, Amsterdam 1989, P. 86.
[31] E. Farjami, L. Clima, K.V. Gothelf, E.E. Ferapontova, DNA interactions with a methylene blue redox indicator depend on the DNA length and are sequence specific, Analyst 135 (2010) 1443-1448.
[32] A. Mudasir, E.T. Wahyuni, D.H. Tjahjono, N. Yoshioka, H. Inoue, Spectroscopic studies on the thermodynamic and thermal denaturation of the ct-DNA binding of methylene blue, Spectrochim. Acta A 77 (2010) 528-34.
[33] Iwona Grabowska, K. Malecka, A. Stachyra, A. Gora-Sochacka, A. Sirko, W. Zagorski-Ostoja, H. Radecka, J. Radecki, Single electrode genosensor for simultaneous determination of sequences encoding hemagglutinin and neuraminidase of avian influenza virus type H5N1, Anal. Chem. 85 (2013) 10167-10173.
[34] Y. Fu, Z. Callaway, J. Lum, R. Wang, J. Lin, Y. Li, Exploiting enzyme catalysis in ultra-low ion strength media for impedance biosensing of avian influenza virus using a bare interdigitated electrode, Anal. Chem. 86 (2014) 1965-1971.
[35] K. Kurzątkowska, A. Sirko, W. Zagorski-Ostoja, W. Dehaen, H. Radecka, J. Radecki, Electrochemical label-free and reagentless genosensor based on an ion barrier switch-off system for DNA sequence-specific detection of the avian influenza virus, Anal. Chem. 87 (2015) 9702-9709.
[36] S. Aydinlik, D. Ozkan-Ariksoysal, P. Kara, A.A. Sayiner, M. Ozsoz, A nucleic acid-based electrochemical biosensor for the detection of influenza B virus from PCR samples using gold nanoparticle-adsorbed disposable graphite electrode and meldola's blue as an intercalator, Anal. Methods 3 (2011) 1607-1614.
[37] S. Dong, R. Zhao, J. Zhu, X. Lu, Y. Li, S. Qiu, L. Jia, X. Jiao, S. Song, C. Fan, R.Z. Hao, H. Song, Electrochemical DNA biosensor based on a tetrahedral nanostructure probe for the detection of avian influenza A (H7N9) virus, ACS Appl. Mater. Interf. 7 (2015) 8834–8842.
[38] A. Bonanni, M.I. Pividori, M. del Valle, Impedimetric detection of influenza A (H1N1) DNA sequence using carbon nanotubes platform and gold nanoparticles amplification, Analyst 135 (2010) 1765-1772.
[39] D-J. Chung, K-C. Kim, S-H. Choi, Electrochemical DNA biosensor based on avidin–biotin conjugation for influenza virus (type A) detection, Appl. Surf. Sci. 257 (2011) 9390-9396.
[40] I. Grabowska, A. Stachyra, A. Gora-Sochacka, A. Sirko, A.B. Olejniczak, Z.J. Lesnikowski, J. Radecki, H. Radecka, DNA probe modified with 3-iron bis(dicarbollide) for electrochemical determination of DNA sequence of Avian Influenza Virus H5N1, Biosens. Bioelectron. 51 (2014) 170-176.

[41] K. Malecka, I. Grabowska, J. Radecki, A. Stachyra, A. Gora-Sochacka, A. Sirko, H. Radecka, Electrochemical detection of avian influenza virus genotype using amino-ssdna probe modified gold electrodes, Electroanalysis 25 (2013) 1871-1878.
[42] H. Fan, P. Ju, S. Ai, Controllable synthesis of CdSe nanostructures with tunable morphology and their application in DNA biosensor of Avian Influenza Virus, Sens. Actuat. B 149 (2010) 98-104.
[43] K. Malecka, A. Stachyra, A. Gora-Sochacka, A. Sirko, W. Zagorski-Ostoja, H. Radecka, J. Radecki, Electrochemical genosensor based on disc and screen printed goldelectrodes for detection of specific DNA and RNA sequences derivedfrom Avian Influenza Virus H5N1, Sens. Actuat. B 224 (2016) 290-297.

Figure legends:

Fig. 1: A FESEM image of the CoO/Pt electrode surface.

Fig. 2: DPVs for MB binding with pDNA, before (red curve) and after hybridization with different concentrations of tDNA (black curves) of 1.0×10^{-15}, 1.0×10^{-14}, 1.0×10^{-13}, 1.0×10^{-12}, 1.0×10^{-11}, 1.0×10^{-10}, and 1.0×10^{-9} mol L^{-1}. Inset: The calibration plot for the dependency of the DPVs peak currents on the tDNA concentration.

Fig. 3: DPVs for MB binding with pDNA, before (red curve) and after hybridization with different concentrations of cDNA (black curves) of 0.5, 1, 2, 4, 8, and 10 ng μL^{-1}. Inset: The calibration plot for the dependency of the DPVs peak currents on the cDNA concentration.

Fig. 4: DPVs for MB binding with pDNA, before and after hybridization with 1.0×10^{-12} mol dm^3 of tDNA, 1miss, 2miss, 3miss and ncDNA sequences.

Fig. 5: DPVs for MB binding with pDNA, before (red curves) and after hybridization with tDNA (green curves) of 1.0×10^{-12} mol L^{-1} for five hybridization/dehybridization cycles.

Table 1: A comparison of the different electrochemical DNA biosensors for influenza virus.

Probe sequence (5'→3')	Influenza subtype/serotype	Redox indicator	Transducer	Detection technique	LOD	Linear range	Real Sample	Remark	Reference
ATTTGGAGCTATAGCAGGTT, AATGGGACTGTCAAAGACAG	H5N1	Mb, Fc	Au	OSWV	18, 21 nM	20-80 nM	-	2 thiolated probes	[33]
GTGTGCATGGATAGCACGTAACGGTGTAGTAGTAA, CGTGCGGGTAGGAAGAAAGGGAAATAGTTGTCGTGTTG	H5N1	Mb	-	EIS	8×10^{-4} HAU in 200 μL	0.001 to 1 HAU	-	Biotinylated aptamer, enzyme	[34]
CCTCAAGGAGAGAGAAGAAG	H5N1	-	Au	OSWV	1.39 pM	1-10 pm	-	Ion barrier switch-off system	[35]
ACCTTCGGCAAAAGCTTCAATACTCCA	B	Meldola's blue	Graphite	DPV	54 pmole	-	PCR samples	Thiolated probe	[36]
-	H7N9	TMB	Au	Amp	100 fM	-	Human	Tetrahedral nanostructure probe	[37]
TGCAGTCCTCGCTCACTGGGCACG	H1N1	-	SPE	EIS	577 pmol L^{-1}	-	-	Biotinylated DNA target, sandwich scheme	[38]
ATGAGTCTTCTAACCGAGGTCGAA	A	Ferro/ferri	GCE	CV	8.51×10^{-14} M	1.0×10^{-13}-1.0×10^{-10} M	-	Avidin-biotin conjugation	[39]
CCTCAAGGAGAGAGAAGAAG	H5N1	-	Au	OSWV	0.08 fM	-	-	3-iron bis(dicarbollide)-modified DNA probe	[40]
CCTCAAGGAGAGAGAAGAAG	H5N1	Ferro/ferri	Au	SWV,EIS	10 fM	-	-	Aminated DNA probe	[41]
GGAATGGTAGATGGATGGTAT	-	MB	CdSe hollow microspheres	DPV	-	-	-	-	[42]
CCTCAAGGAGAGAGAAGAAG	H5N1	Ferro/ferri	Au	OSWV	10 pM	-	-	Thiolated probe	[43]

GGTTTTGGCCAGCACTACAGC	A	MB	CoO nanoflakes	DPV	86.4 amol L^{-1}	1.0 fmol L^{-1} to 1.0 nmol L^{-1}	Cultured samples, Human subjects	No probe modification, no tag, no label	This work

Abbreviations:
LOD: limit of detection
Mb: methylene blue
Fc: ferrocene
OSWV: Osteryoung square-wave voltammetry
EIS:
HAU: hemagglutination units
Amp: Amperometry
TMB: 3,3',5,5'-Tetramethylbenzidine
SPE: screen printed electrode
Ferro/ferri: Ferrocyanide/ferricyanide redox couple
GCE: Glassy carbon electrode
SWV: square-wave voltammetry

Table 2: The concentrations of cDNA in the human samples obtained by the biosensor and based on optical densities at 260 and 280 nm.

Sample	cDNA obtained by optical density measurements / ng μL^{-1}	cDNA obtained by the biosensor / ng μL^{-1}
Positive 1	2420.3	1128
Positive 2	2296.8	1230
Positive 3	2127.4	1228
Positive 4	2270.1	1317
Positive 5	2166.8	1409
Positive 6	2423.1	1299
Positive 7	2007.5	1687
Negative 1	438	-*
Negative 2	591	-*
Negative 3	593.5	-*
Negative 4	1076	-*

*No significant signal was detected, after hybridization of the biosensor with this sample.

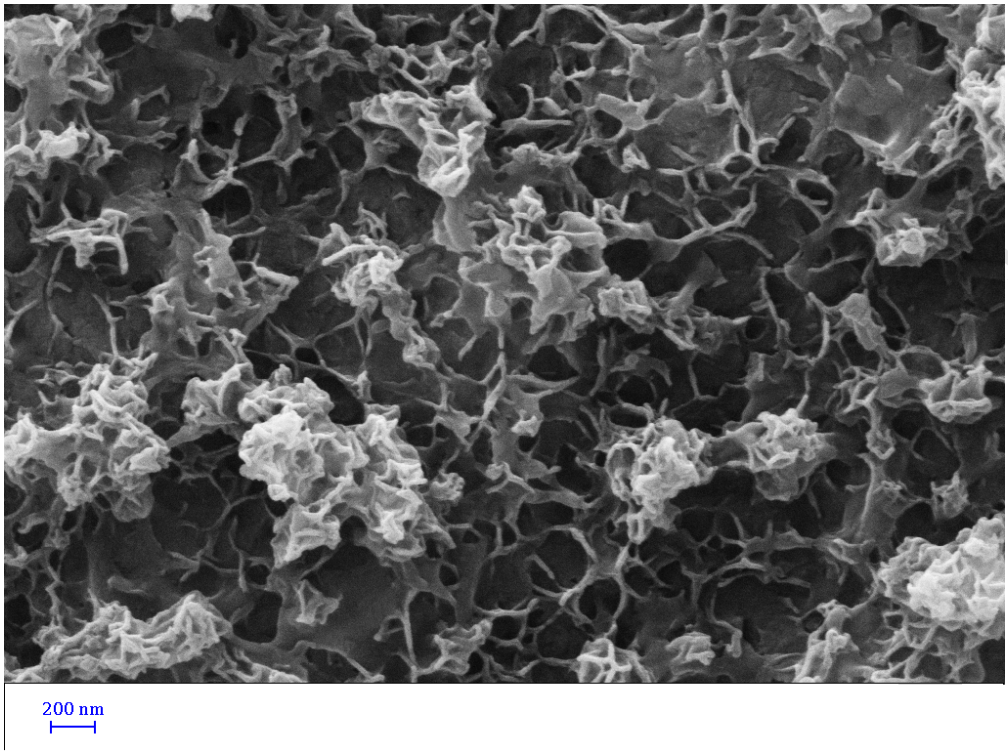

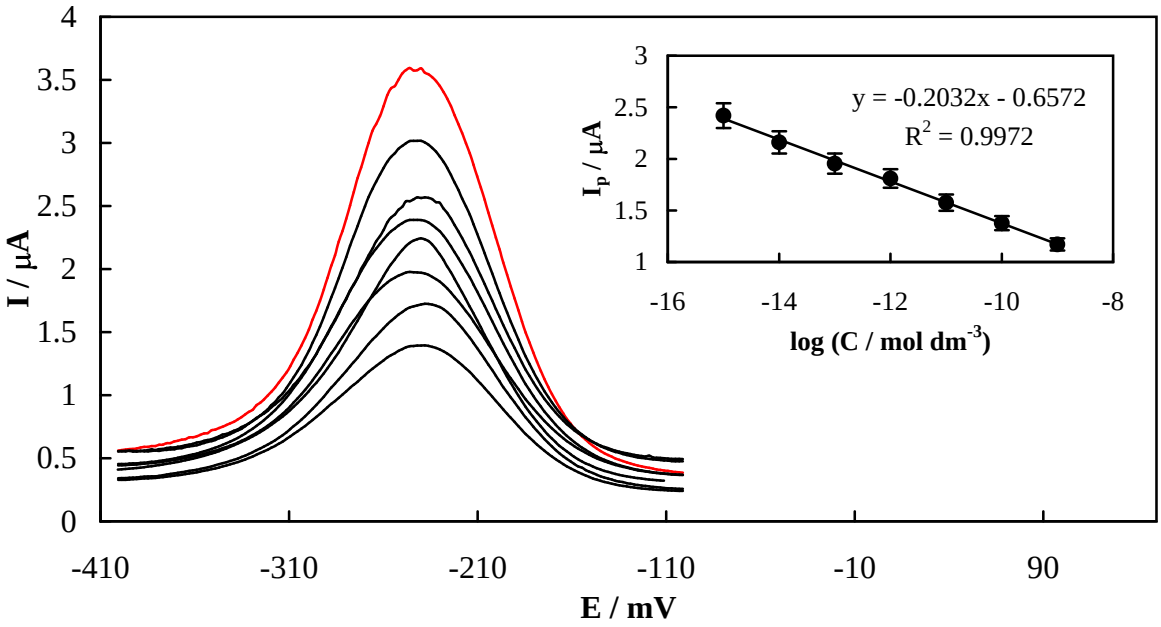

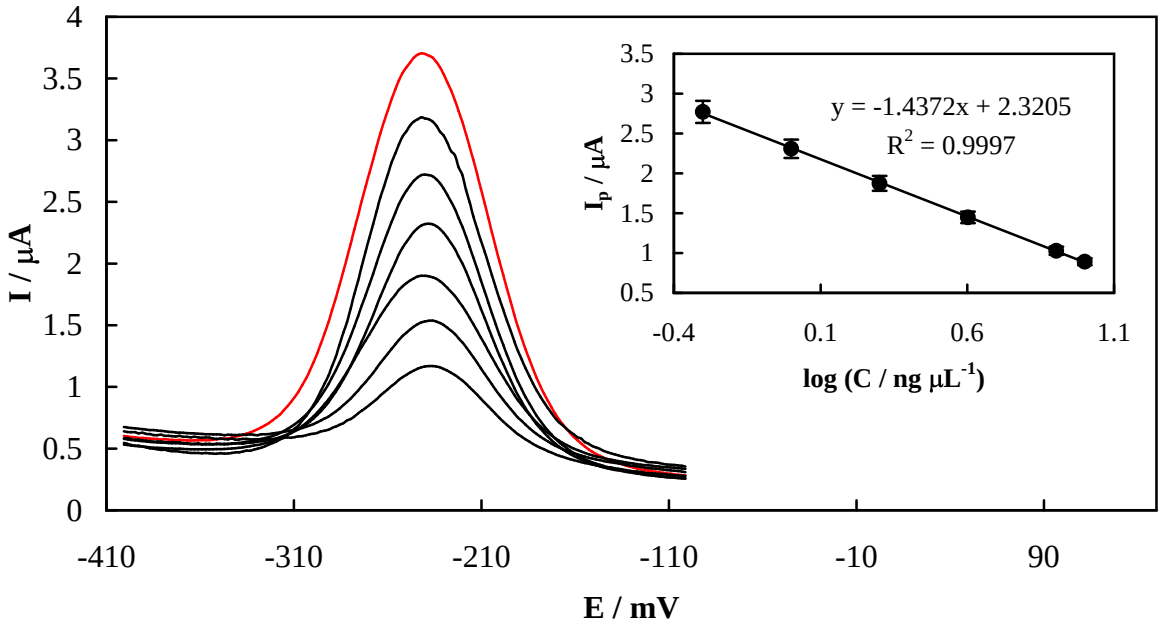

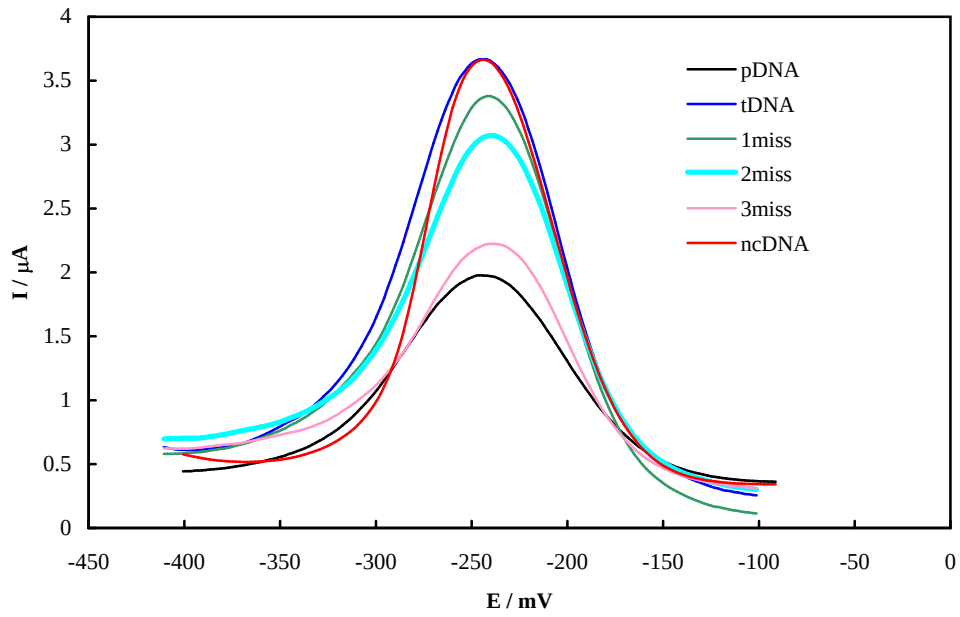

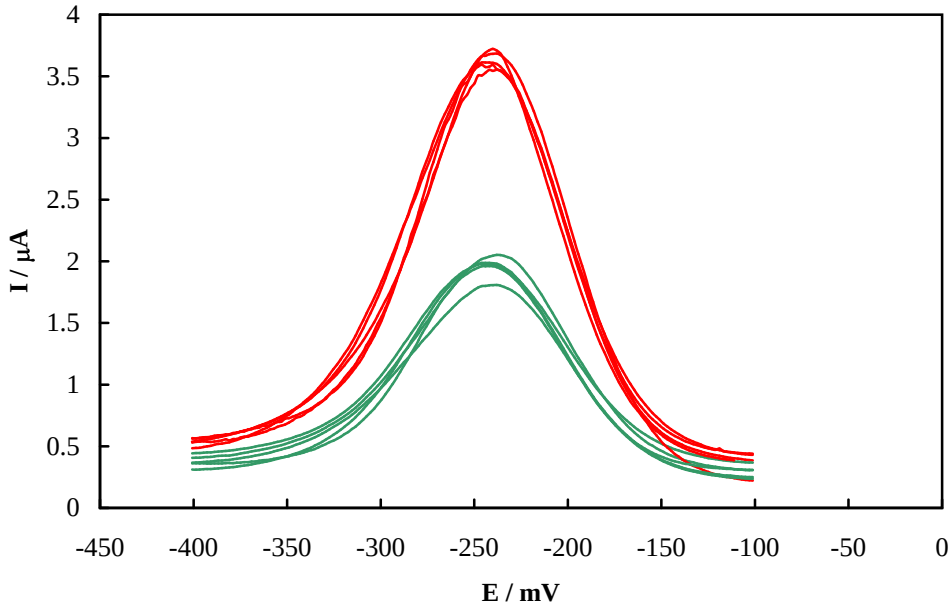

Highlights:

- Meso/macroporous cobaltous oxide nanoflakes were electrodeposited.
- The nanoflakes were employed to fabricate an influenza biosensor.
- The biosensor was applied to detect clinical samples.